4.3.5 Step 4 (Local improvement): Po Plain cold/hot pool

• Po plain grid: Po Plain area from *USGS GTOPO30 DEM*

As described in *Spinoni et al. (2008)*, it is well known that the Po Plain is a cold region in winter and a hot one in summer because of the quite total absence of winds and due to the Po Plain being locked by the Alps and the Apennines.

With a Fortran code we isolated the Po Plain and we created a "Po Plain grid" where the Po Plain grid cells were labelled with "1" and every other cell was assigned "0".

A grid cell belongs to Po Plain if all the conditions below are satisfied:
- it is within the geographical limits given by hand-made borders obtained with ArcGIS™ tools (*ArcGIS website*) ;
- the elevation is lower than 300 m ;
- at most 20 of the surrounding 120 grid cells (11 km x 11 km) are 50 m higher than the considered grid cell;
- the slope must be lower than 50m/km.

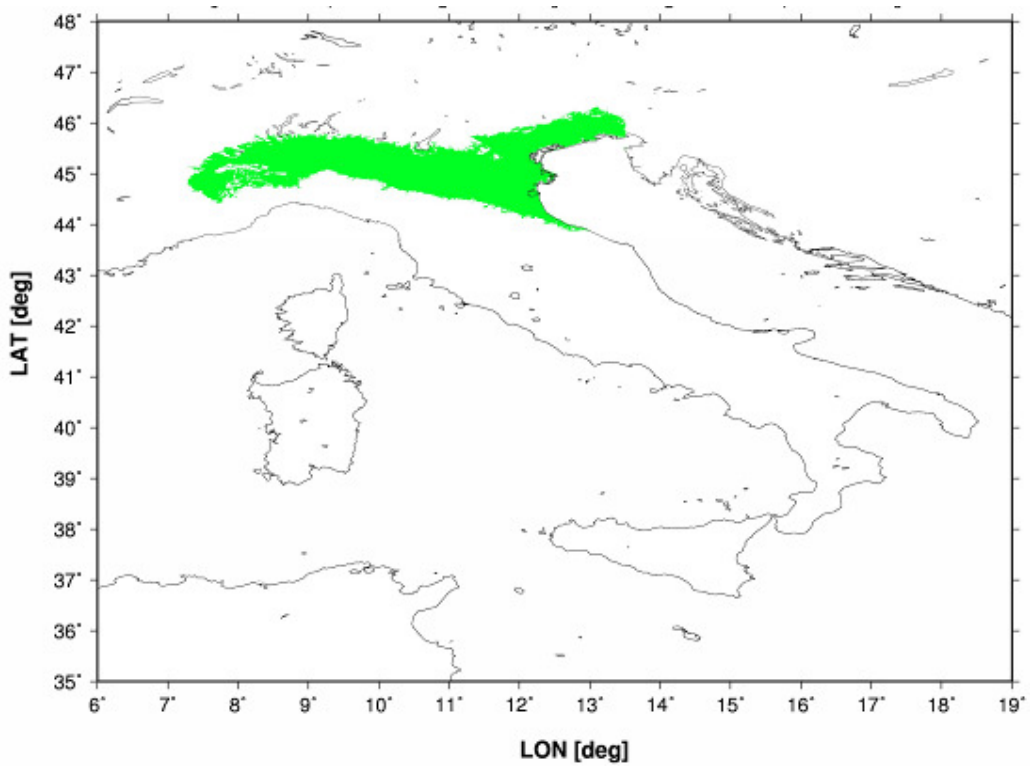

Fig.45 The Po Plain area as used in our temperature models.

• Mean Temperature

We selected 142 T_M stations that are located within the Po Plain raster grid limits; we studied their residual and we found that almost every station shows negative residuals in winter and positive residuals in summer. The Po Plain influence is effective up to Venice, then it rapidly vanishes to no effect at 13.5 °E, thus we modelled it with a smoothing (a linear smoothing that soften the effect going eastward) between 13 °E and 13.5 °E.

The Po plain effect is monthly modelled as:

$$PO_M(POGRID_{DEM}) = \left(\overline{RESTM_{MLR+SEA+LAKE}}\right)_{POPLAINSTATIONS} \quad \textbf{(79)}$$

Here they are the monthly coefficients used for the Po Plain effect on T_M:

(°C)	AVG
JAN	-0.92
FEB	-0.60
MAR	-0.28
APR	0.00
MAY	0.19
JUN	0.37
JUL	0.38
AUG	0.31
SEP	0.21
OCT	-0.03
NOV	-0.42
DEC	-0.73

Tab.15 Monthly coefficients for Po Plain effect on T_M

As expected, the Po Plain is a cold pool in winter (approximately -0.9 °C in January) and a hot pool in summer (approximately 0.4° C in July). Such values are the averaged 1961-1990 values, thus they should not be confused with the summer heat waves, for example, that are felt more intensively in the Po Plain rather than in the areas next to the Alps.

In the end, we added back the Po plain effects to the modelled *MLR* plus the sea and plus the lake effects T_M as:

$$TM4_M = TM3_M + PO_M \quad \textbf{(80)}$$

• Minimum Temperature

For T_N we used the same methodology used for T_M, but we studied the residuals of 130 stations.

Here they are the coefficients used for the Po Plain effect on T_N:

(°C)	AVG
JAN	-0.68
FEB	-0.51
MAR	-0.28
APR	0.01
MAY	0.31
JUN	0.50
JUL	0.59
AUG	0.52
SEP	0.36
OCT	0.12
NOV	-0.21
DEC	-0.60

Tab.16 Monthly coefficients for Po Plain effect on T_N

As for T_M, the Po Plain effect is a cooling effect for T_N in winter months (-0.7 °C in January) and a warming effect for T_N in summer months (0.6 °C in July).

• Maximum Temperature

The same considerations made for T_N hold for T_X.

In the next page, in table 17, we show the coefficients used for the Po Plain effect on T_X.

(°C)	AVG
JAN	-1.25
FEB	-0.91
MAR	-0.61
APR	-0.39
MAY	-0.30
JUN	-0.24
JUL	-0.41
AUG	-0.46
SEP	-0.38
OCT	-0.49
NOV	-0.78
DEC	-1.01

Tab.17 Monthly coefficients for Po Plain effect on T_X

For T_X, the Po Plain effect is always a cooling effect, more significant in winter months (approximately -1.3 °C in January) than in summer months (-0.4 °C in July) or in spring months (-0.3 °C in May).

- **Improvements and evaluation of the Residuals after Po Plain correction**

Let us show the T_M January and July maps after the modelling of the Lake and the Po Plain effects.

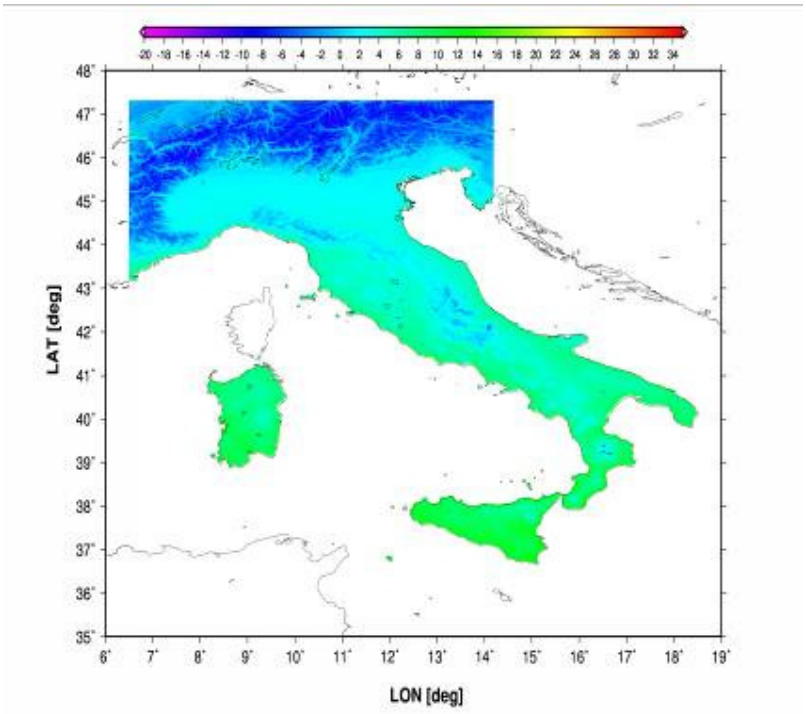

Fig:46 January 1961-90 T_M map after MLR model plus the sea, lake and Po plain effects improvements (°C

)

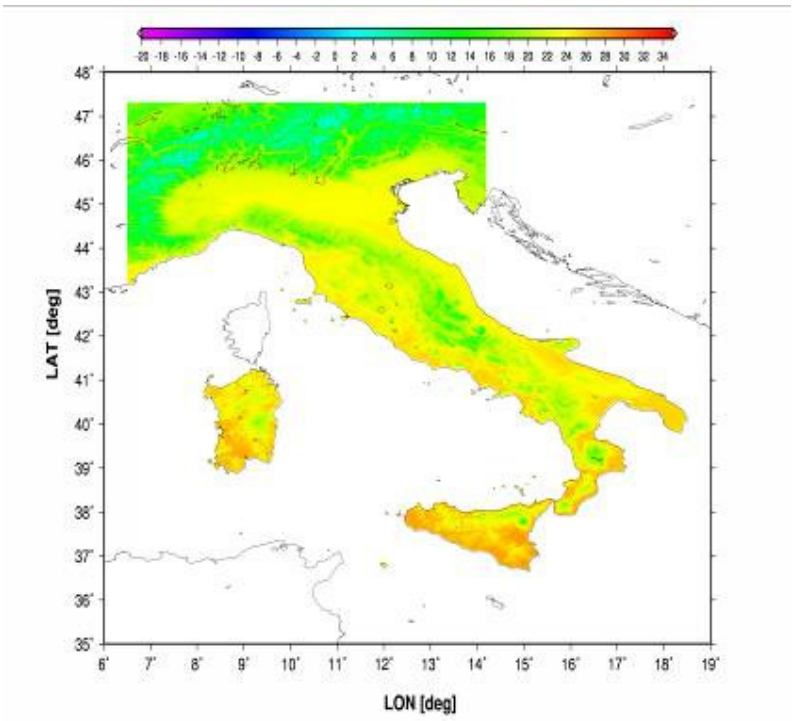

Fig.47 July 1961-90 T_M map after MLR model plus the sea, lake and Po plain effects improvements (°C)

Once again, residuals were calculated as:

$$RESTM_{MLR+SEA+LAKE+PO} = RESTM_{MLR+SEA+LAKE} - PO_M(POGRID_{DEM}) \quad \textbf{(81)}$$

The same holds for T_N and T_X.

The next table shows the statistical parameters after the Po Plain effect.

After PO PLAIN	***AVG***	***-0.04***	***1.11***	***1.40***		***AVG***	***0.01***	***0.84***	***1.06***		***AVG***	***0.10***	***1.06***	***1.36***
After Lake	***AVG***	***-0.04***	***1.11***	***1.41***		***AVG***	***-0.01***	***0.85***	***1.07***		***AVG***	***0.03***	***1.07***	***1.38***
IMPROVEMENT	***AVG***	***0.00***	***0.00***	***0.01***		***AVG***	***0.00***	***0.00***	***0.01***		***AVG***	***-0.07***	***0.01***	***0.02***

Tab.18 Yearly averaged statistical error values after Po Plain corrections and comparisons (°C)

As for the lake effect, the Po Plain effect introduced small improvements, but it is an important local refinement that here was modelled in a more realistic way than in *Spinoni et al. (2008)* and in *Hiebl et al. (2009)*.

4.3.6 Step 5 (Global improvement): solar radiation anomaly

• Solar radiation grids: monthly global radiation from solar radiation climatologies for Italy (see Chapter 6)

The basic idea of this step is that temperatures and solar radiation are correlated variables, but only a few climate models *(*e.g. *Ninyerola et al., 2007)* use solar radiation as an independent variable in temperature models.

This is due to many reasons: solar models are usually based only on topographic and astronomical parameters. Thus no real information is provided for a particular time interval as 1961-1990. In addition, because of a wide lack of solar radiation stations, global radiation data are usually difficult to be obtained at a spatial high resolution. Also, indirect measurements as sunshine durations or cloudiness observations are usually not reliable or insufficient for high-resolution models.

In Italy, sunshine duration records have been available since approximately 1950. Thus we decided to realize a solar model for Italy based on real data plus topographic and astronomical parameters (see Chapter 6 for details). We realized 1961-1990 direct, diffuse, reflected, global and absorbed radiation grids (with the same resolution of *USGS DEM*) for Italy, starting from 1961-1990 sunshine duration station data.

The monthly 1961-1990 global, direct and absorbed solar radiation maps, with data expressed in MJ/m^2, are shown in Chapter 6; the gridded data for all the solar radiation variables can be obtained by request.

We did not use the global radiation as a predictor for our temperature models, but we calculated, for each grid cell, the global radiation anomaly, that is the difference between the global radiation received from the grid cell and the surrounding 2,500 km^2. This is because latitudinal effect included in global radiation grids were already de-trended in temperature models and residuals:

$$AnRad_{CELL} = GlobRad_{CELL} - \overline{GlobRad_{CELL}}\Big|_{2500km^2} \quad \textbf{(82)}$$

Where $AnRad_{CELL}$ is the radiation anomaly for the considered grid cell.

Thus, e.g., a northward facing grid cell has a negative solar radiation anomaly if the surrounding cell is heterogeneously distributed for aspect. On the contrary, a southward

facing grid cell has a positive solar radiation anomaly if the surrounding cell is heterogeneously distributed for aspect.

Let us see the global radiation anomaly map for January (the values are expressed in MJ/m^2 and are referred to the average day in January):

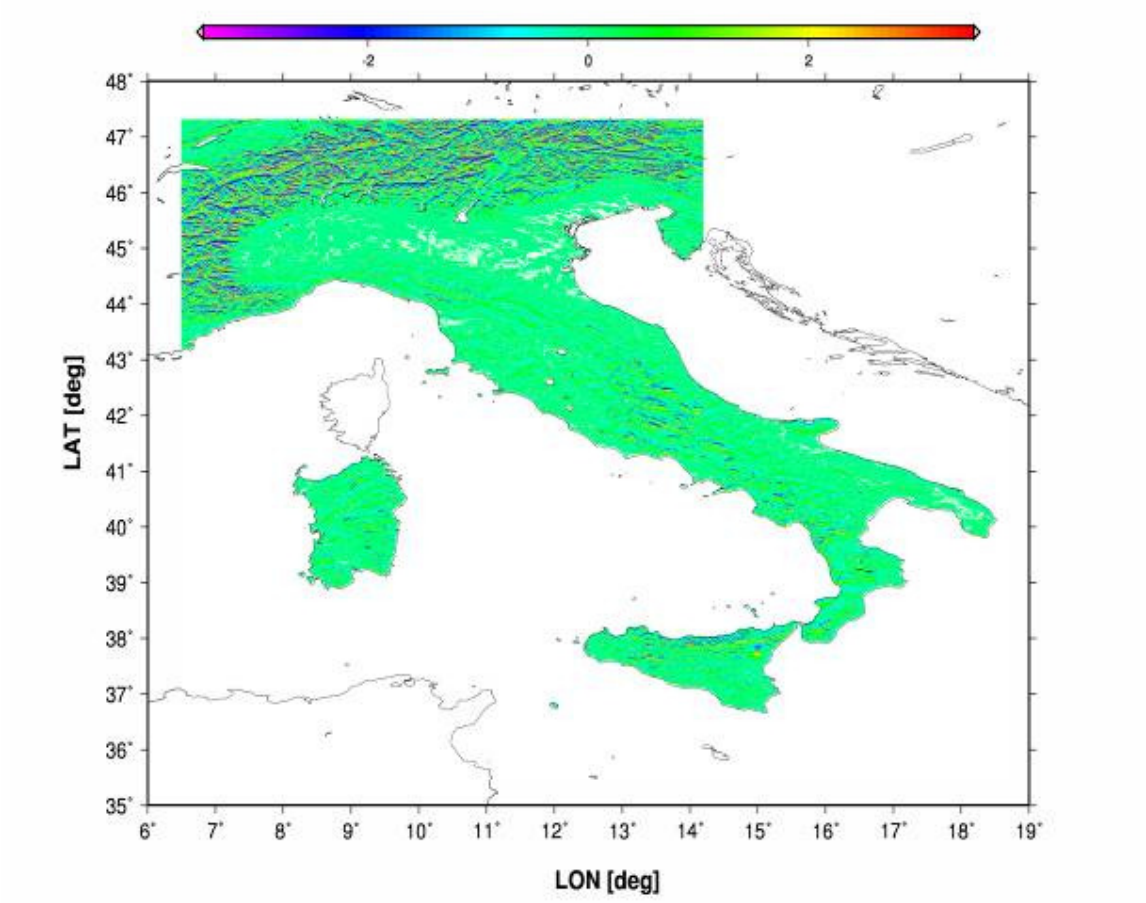

Fig.48 January 1961-90 Global Solar Radiation Anomaly map (°C)

In fig. 48, the white regions in Italy mean that the anomaly was lower, in absolute values, than 0.1 MJ/m^2day.

• Mean Temperature

The main problem to overcome is the resolution of the *DEM*. A temperature station is usually located in a very small surface and it is located in plain grounds, far from obstacles as mountain ridges or hills. On the other hand, the *DEM* provides, for each grid cell, the

average value of elevation, slope, aspect (the last two parameters were calculated, not given, see Chapter 5 for details) and so on for a squared kilometre. Thus we can assign to a station a slope value of, e.g., 120 m/km for the corresponding cell, whilst the station is on a flat area.

These facts cause problems if we want to model temperature versus solar radiation. Shadowing and overshadowing effects, different behaviour of, e.g., northward facing surfaces (grid cells in our case) versus southward facing ones and so on, are all peculiarities included in the anomaly grids, but the station could not be well represented by such processes mainly because of resolution problems described above.

Thus, we decided to perform our residual analysis only on stations located in the Alps, that is on 348 stations, and we calculated a transfer coefficient between T_M and global radiation anomalies:

$$RESTM\Big|_{eq81} = \alpha \cdot AnRad_{STATIONS} \qquad \textbf{(83)}$$

Where the residuals are from equation (81) and α is the transfer coefficient measured in °C/(MJ/m²): if a station is in a cell with a positive radiation anomaly, it receives more radiation than the average radiation and it should show higher temperatures.

Then we applied the transfer coefficient to every Italian grid cell:

$$SUN_M(AnRadGrid_{DEM}) = \alpha \cdot AnRad_{DEM} \qquad \textbf{(84)}$$

Here we are the monthly α coefficients used for the solar radiation effect on T_M:

°C/MJ/m²	α
JAN	0.18
FEB	0.09
MAR	-
APR	-
MAY	-
JUN	-
JUL	-
AUG	-
SEP	0.01
OCT	0.09
NOV	0.18
DEC	0.24

Tab.19 Monthly anomaly transfer coefficients for solar radiation on T_M

As we can see, no significant effects were found for spring and summer months. Obviously, this value is a 30-year average and it takes intrinsically into account cloudiness, diffuse and reflected radiation other than direct radiation, consequently it is a small value. Furthermore, the inexact collocation of many stations can lead to biased results, but this step can surely be improved in future works.

In the end, we added back the solar radiation effects to the modelled *MLR*, plus sea, lake and Po Plain effects on T_M as:

$$TM5_M = TM4_M + SUN_M \quad \textbf{(85)}$$

• Minimum Temperature

The same methodology used for T_M was used for T_N, but 275 T_N were used to calculate the monthly α coefficients that, in this case, are:

°C/MJ/m²	α
JAN	0.33
FEB	0.26
MAR	0.22
APR	0.19
MAY	0.23
JUN	0.28
JUL	0.35
AUG	0.27
SEP	0.23
OCT	0.19
NOV	0.28
DEC	0.37

Tab.20 Monthly anomaly transfer coefficients for solar radiation on T_N

For T_N the solar radiation effect is significant for all months: e.g., in December, a grid cell that has a radiation anomaly of 3 MJ/m² is consequently given a warming effect of approximately 1.1 °C.

Let us show, in fig. 49, an example: January solar radiation effect on T_N (values expressed in °C):

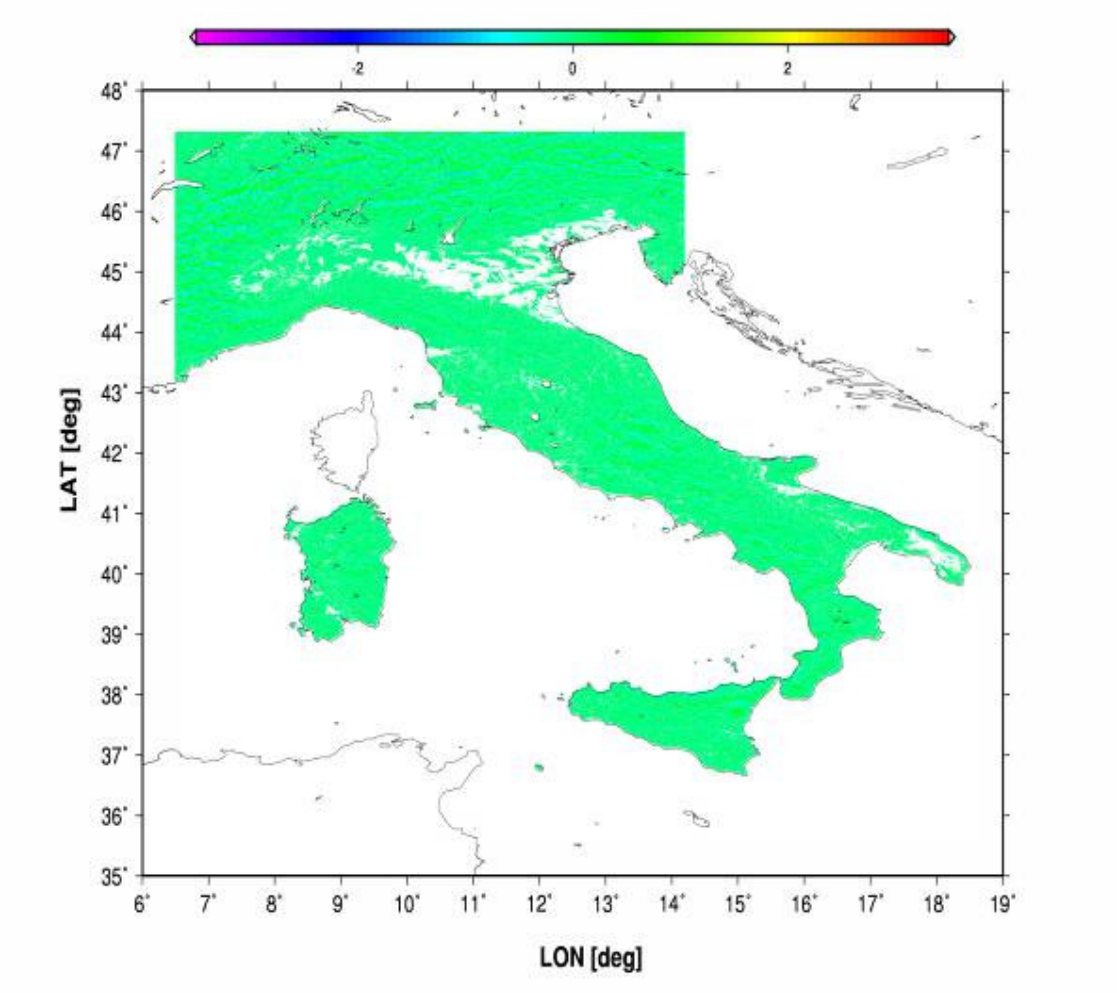

Fig:49 January 1961-90 solar radiation effect map (°C)

As we can see in fig. 49, the plains are slightly modified by radiation effects, as expected.

• Maximum Temperature

The same considerations made for T_N holds for T_X, here the monthly α coefficients are the one shown in table 21 (see the next page).

℃/MJ/m²	α
JAN	0.183
FEB	0.091
MAR	-
APR	-
MAY	-
JUN	-
JUL	-
AUG	-
SEP	-
OCT	-
NOV	0.183
DEC	0.276

Tab.21 Monthly anomaly transfer coefficients for solar radiation on T_X

For T_X, the solar radiation effect is significant only in winter months, but lower than for T_N and T_M.

• Improvements and evaluation of the Residuals after solar radiation effect

Once again, residuals were calculated as:

$$RESTM_{MLR+SEA+LAKE+PO+SUN} = RESTM_{MLR+SEA+LAKE+PO} - SUN_M(AnGrid_{DEM}) \qquad \textbf{(86)}$$

The same holds for T_N and T_X. The next table shows the statistical parameters after the solar radiation effect:

After Radiation	AVG	-0.03	1.09	1.39		AVG	0.01	0.84	1.06		AVG	0.10	1.06	1.36
After Po Plain	AVG	-0.04	1.11	1.40		AVG	0.01	0.84	1.06		AVG	0.10	1.06	1.36
IMPROVEMENT	AVG	0.01	0.02	0.01		AVG	0.00	0.00	0.00		AVG	0.00	0.00	0.00

Tab.22 Yearly averaged statistical error values after solar radiation corrections and comparisons (℃)

Let us underline an important fact: this modelled effect reproduces the differences caused by a different received global solar radiation with strong physical-based motivations, but when the residual evaluation after this effect are evaluated, the improvements are very small. This is mainly due to the fact that the stations are located in flat grounds and far from shadowing obstacles. Thus, the small improvements in the statistical parameters mark the need of a higher resolution *DEM* (*50* m x *50* m would be better) in order to model the solar radiation dependence of temperature.

4.3.7 Step 6 (Global improvement): macro-aspect parameterization

• Slope orientation grid: Macro-Aspect grid from USGS GTOPO30 DEM

In physical geography, aspect generally refers to the horizontal direction to which a mountain slope faces; thus it is generally expressed as an angular term. It is well known *(Hiebl et al., 2009; Daly et al., 2009; Bennie et al., 2006)* that different facing surfaces behave differently related to climate variables. For example, *Bolstad et al. (1998)* found, in long time averages, that a north-east facing surface is 1.4 °C cooler than a south-west facing one and this value can dramatically increase up to 10 °C for daily extreme values.

By means of a Fortran code, we smoothed the *USGS DEM*. For every grid cell, we substitute the average elevation of the 400 surrounding cells (i.e. over the surrounding 400 km^2) to the cell's own elevation. Then we calculated the smoothed aspect just considering the 4 grid cell at 10 km (following the straight lines towards the cardinal points) from the grid cell under investigation.

Here we show the "macro-aspect" map from the gridded data, 0 rad (and 6.28 rad) refers to south, going counter-clockwise, 1.57 rad refers to west, 3.14 rad to north and 4.71 rad to east.

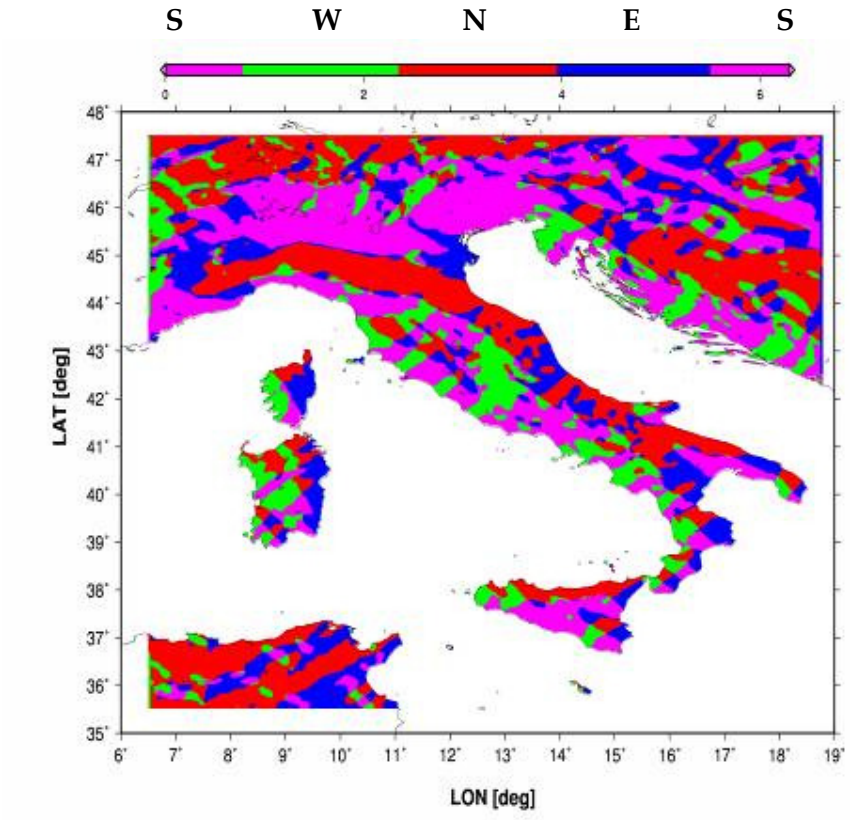

Fig.50 Macro-Aspect raster map (rad): violet is for south, green is for west, red is for north, blue is for east

• Mean Temperature

We used a smoothed version of the common aspect grids because of the inaccurate (and the different scales as seen in former paragraphs) geo-referencing of the stations. Whilst we supposed that the dependence of temperature on aspect might be captured, for example, by separating the stations facing north from those facing south across a mountain ridge.

First, we assigned to each station the "macro-aspect" value of the raster grid. Then we performed our residual analysis on every station except of stations located at less than 1 km from the sea's coast.

We used a polynomial model that uses the residuals obtained from equation (86) versus the aspect of the corresponding grid cell (where the station is located):

$$RESTM\big|_{eq.86}\ (Asp_S) = \alpha \cdot Asp_S^4 + \beta \cdot Asp_S^3 + \gamma \cdot Asp_S^2 + \delta \cdot Asp_S + \varepsilon \qquad \textbf{(87)}$$

Here they are the seasonal coefficients used for the macro-aspect effect on T_M:

	α	β	γ	δ	ε
winter	*-0.0039*	*0.0621*	*-0.2905*	*0.3521*	*0.0970*
spring	*-0.0066*	*0.0858*	*-0.3290*	*0.3191*	*0.0779*
summer	*-0.0076*	*0.0936*	*-0.3320*	*0.2851*	*0.0455*
fall	*-0.0047*	*0.0676*	*-0.2899*	*0.3186*	*0.0853*

Tab.23 Seasonal polynomial coefficients for macro-aspect model on T_M

In tab. 23, the winter months are December, January and February, the spring months are March, April and May, the summer months are June, July and August, the fall months are September, October and November.

The coefficients were calculated using the macro-aspect of all the stations (apart from those located less than 1 km from the sea) and then applied to every Italian grid cell as:

$$Asp_M = \alpha \cdot Asp_{DEM}^4 + \beta \cdot Asp_{DEM}^3 + \gamma \cdot Asp_{DEM}^2 + \delta \cdot Asp_{DEM} + \varepsilon \qquad \textbf{(88)}$$

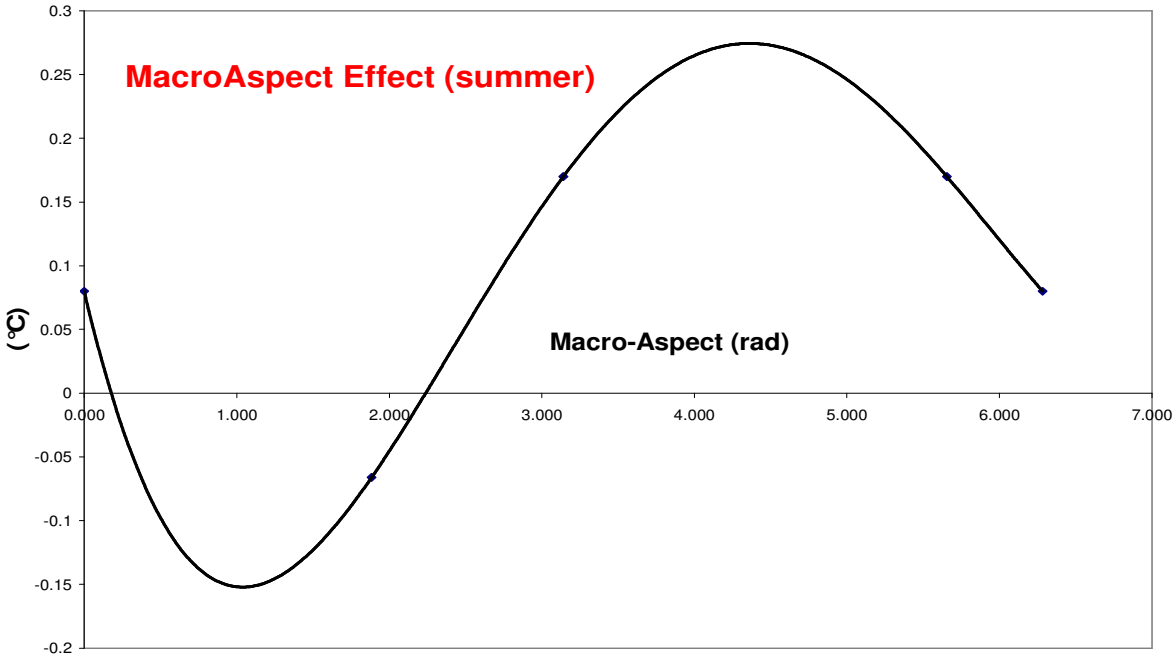

Fig.51 Macro-Aspect polynomial model for summer months: effect in °C versus aspect in rad

As we can see, this modelled effect warms up S and S-W and S-E slopes, whilst it cools up the slopes that face towards north, as expected. In summer, e.g., the maximum difference in absolute values is approximately 0.4 °C.

In the end, we added back the macro-aspect effects to the T_M modelled with *MLR* plus sea, lake, and solar radiation effects as:

$$TM6_M = TM5_M + Asp_M \quad \textbf{(89)}$$

• Minimum Temperature

The same methodology used for T_M was used for T_N and even the same coefficients, because the residual analysis yielded quite identical results.

In the next page, in fig. 52, we show an example map: January macro-aspect effect map for T_N.

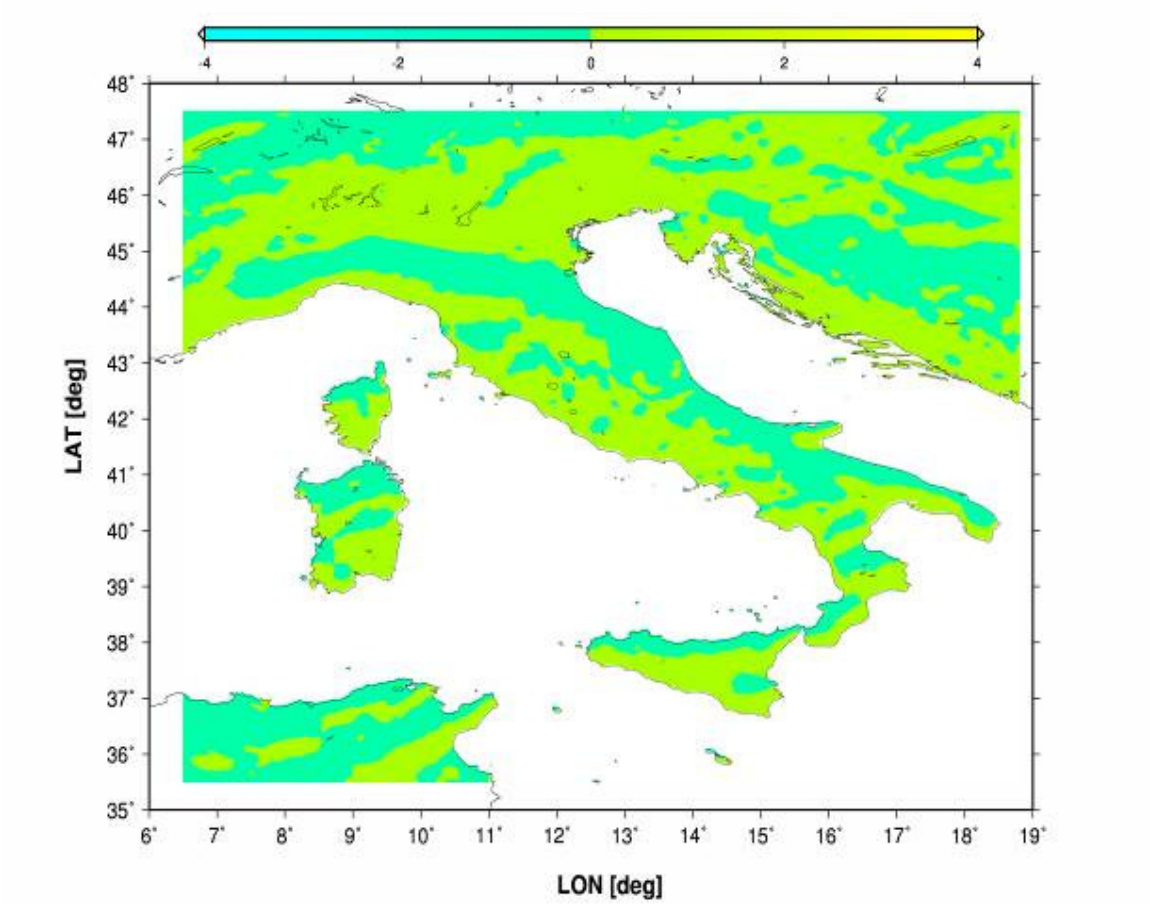

Fig.52 Summer Macro-Aspect effect map: green for negative anomalies, yellow-green for positive ones (°C)

• Maximum Temperature

The same considerations made for T_N are valid for T_X.

• Improvements and evaluation of the Residuals after macro-aspect effect

Once again, the residuals were calculated as:

$$RESTM_{MLR+SEA+LAKE+PO+SUN+ASP} = RESTM_{MLR+SEA+LAKE+PO+SUN} - Asp_M \qquad \textbf{(90)}$$

The same holds for T_N and T_X. The next table shows the statistical parameters after the macro-aspect effect evaluation.

Post Macro-Asp	***AVG***	***-0.06***	***1.10***	***1.40***		***AVG***	***-0.02***	***0.83***	***1.06***		***AVG***	***0.07***	***1.04***	***1.35***
Post Solar Rad	***AVG***	***-0.03***	***1.09***	***1.39***		***AVG***	***0.01***	***0.84***	***1.06***		***AVG***	***0.10***	***1.06***	***1.36***
IMPROVEMENT	***AVG***	***-0.03***	***-0.01***	***-0.01***		***AVG***	***-0.01***	***0.01***	***0.00***		***AVG***	***0.03***	***0.02***	***0.01***

Tab.24 Yearly averaged statistical error values after macro-aspect corrections and comparisons (°C)

The introduction of the macro-aspect effect leads to small improvements, but even in this case, this is a realistic (as reported in literature) effect that improves the model without improving the statistical error parameters because they are calculated on the stations.

4.3.8 Step 7 (Global improvement): summit-valley *LR* model

• Summit-Valley grid: "*NCEL*" grid from USGS GTOPO30 DEM

In order to study the effects on temperatures caused by narrow or large valleys and by summit locations, we created, with the help of a Fortran code, a raster that characterizes a "summit-valley" continuous coefficient, not just a binary coefficient "yes" or "no".

We defined the "*NCEL*" parameter as:

$$NCEL = \frac{Xcells}{Ycells} \qquad \textbf{(91)}$$

Where *Xcells* is the number of the cells among the surrounding 120, while "not sea cells", whose elevation is at least 50 m lower than that of the cell under consideration. *Ycells* is the number of "not sea cells" out of the surrounding 120 cells. If NCEL = 1 every "not sea cell" in the surrounding 120 km² has an elevation at least 50 m lower than the elevation of the investigated cell, if NCEL = 0 every "not sea cell" in the surrounding 120 km² has an elevation 50 m higher less than the investigated cell. In simpler words, if NCEL > 0.8 the cell is a top cell, if NCEL < 0.2 the cell is in a valley, if NCEL < 0.1 the cell is in a narrow valley and NCEL = 0 represents coasts or plains.

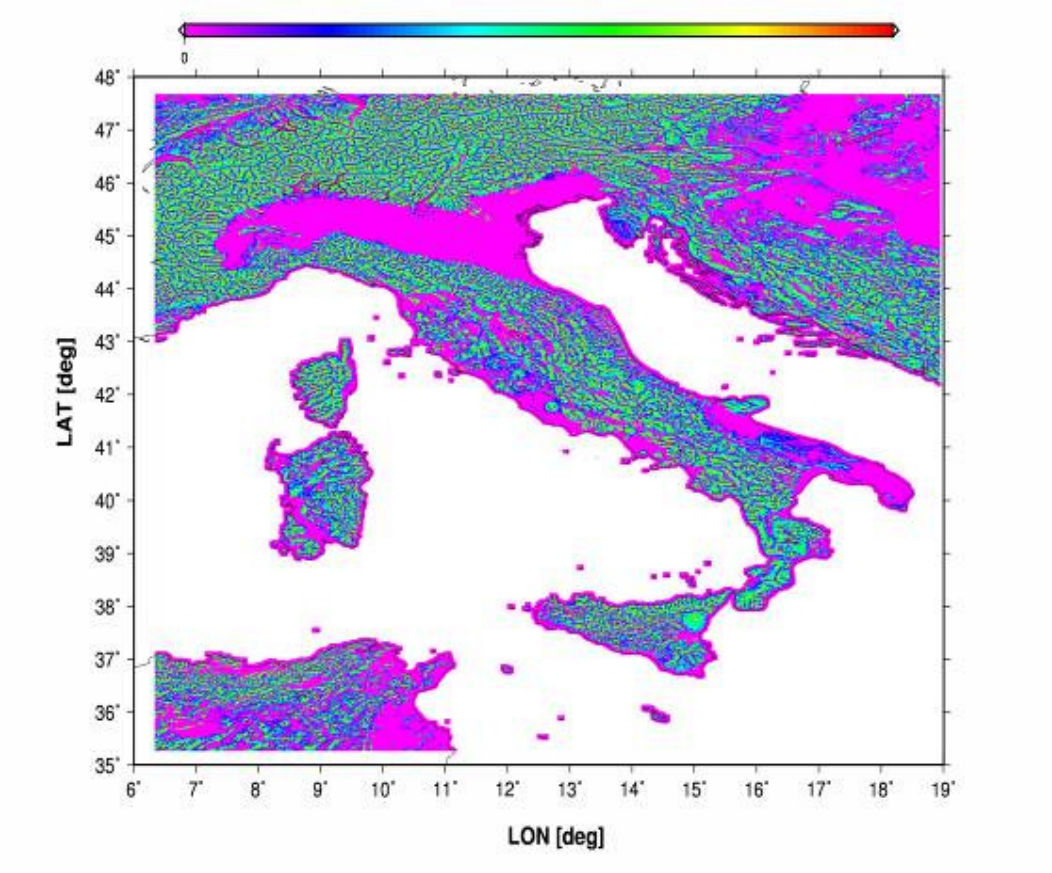

Fig.53 NCEL summit-valley raster grid (NCEL ranges from 0, violet, to 1, red)

• Mean Temperature

The complicated climate features of deep valleys are well documented in literature: the low-level thermal inversions *(Chutko et al., 2009)*, the cold winter air pool structures and evolution in narrow valleys and sinks *(Clements et al., 2003)*, the formation and the destruction of such inversion layers in valleys, the surface energy budget in deep valleys *(Whiteman et al., 1989a-b)*. Usually, the valleys are expected to be colder than the surrounding areas in winter and warmer in summer because of air masses stagnating and also because of inversion layers.

On the other hand, the summit effect was not frequently studied, but we know that a summit is subjected to many phenomena. The principal energy source of Earth is solar radiation, thus a top station should be warmer, but we know (the lapse rates of temperature versus elevation are evident proofs) that the air is "warmed" partly from the

ground, thus a top should be colder. In addition, the winds should be taken into account dealing with exposed and high peaks and so on.

From the residuals, we inferred that a linear regression model for the *NCEL* parameter explains in a satisfactory way both valley and top effects in a unique model (12 monthly models for each variable), provided that we exclude from the *LR* model calculations the stations that are at less than 15 km from the coast.

We used an *LR* model using the residuals obtained from step 6, after having assigned a *NCEL* value to each station, that is:

$$RESTM\ (NCEL)\Big|_{eq.90} = a \cdot NCEL + b \qquad \textbf{(92)}$$

Here they are the monthly coefficients used for the summit-valley on T_M:

	a	*b*
JAN	*0.45*	*-0.07*
FEB	*0.34*	*-0.04*
MAR	*0.24*	*-0.03*
APR	*0.31*	*-0.07*
MAY	*0.37*	*-0.11*
JUN	*0.49*	*-0.16*
JUL	*0.64*	*-0.20*
AUG	*0.64*	*-0.20*
SEP	*0.46*	*-0.13*
OCT	*0.35*	*-0.08*
NOV	*0.35*	*-0.07*
DEC	*0.54*	*-0.11*

Tab.25 Monthly coefficients for top valley model for T_M

As we can infer from tab. 25, an "isolated summit" is subjected to a warming effect of 0.43 °C in December, whilst a "pothole valley" is subjected to a cooling effect of -0.11 °C in the same month.

The coefficients were then applied to every Italian grid cell except of the cells at a distance from the coast lower than 15 km, according to the sea distance raster grid:

$$TV_M\ (NCEL_{DEM}) = a \cdot NCEL_{DEM} + b \qquad \textbf{(93)}$$

In the end, we added back the summit-valley effects to the T_M modelled with *MLR* plus the sea, lake, Po Plain, solar radiation, and Macro-Aspect effects as:

$$TM7_M = TM6_M + TV_M \quad \textbf{(94)}$$

Let us show January and July maps after top valley effects:

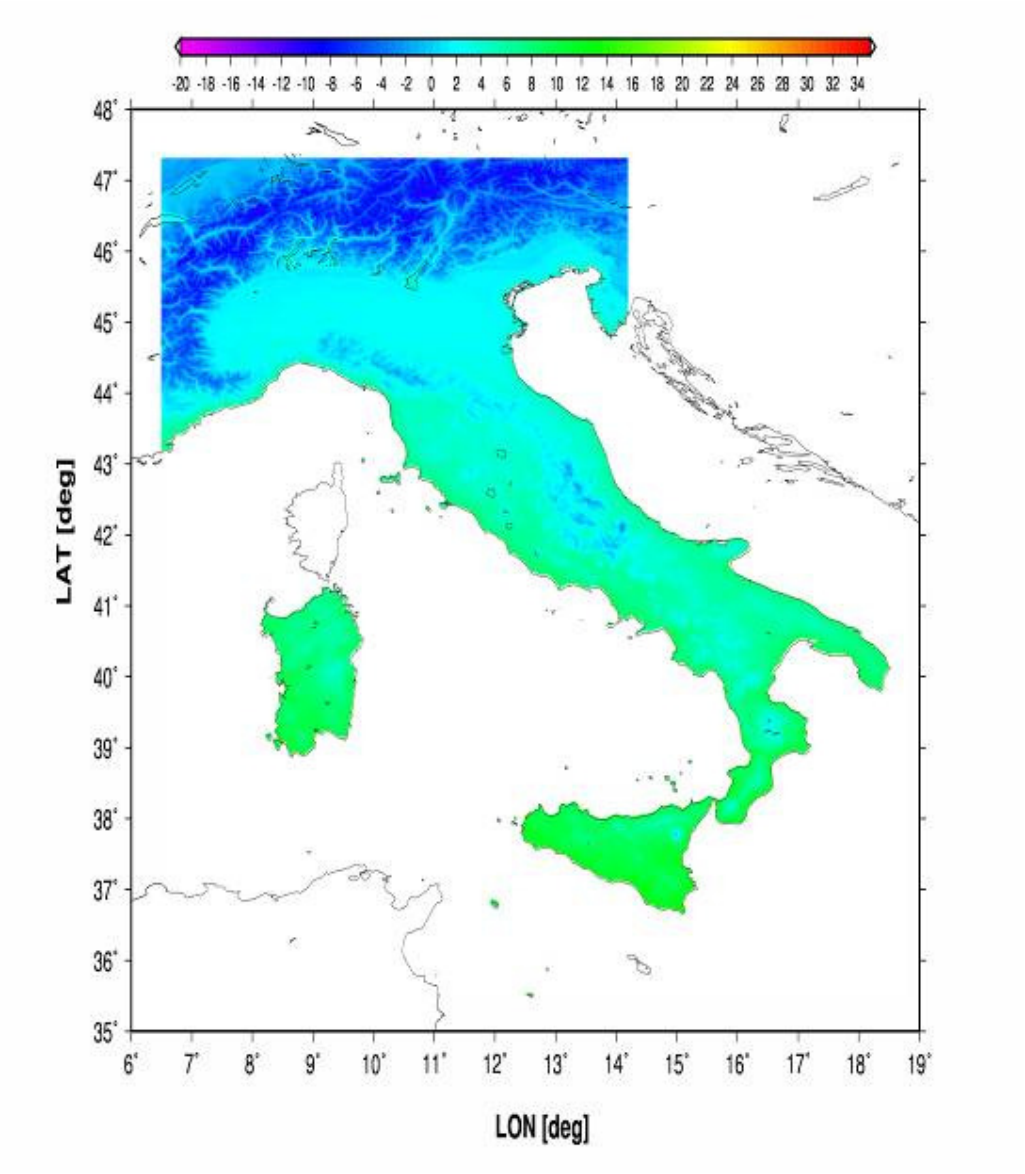

Fig.54 January 1961-90 T_M map after top valley effect and all the former modelled effects (°C)

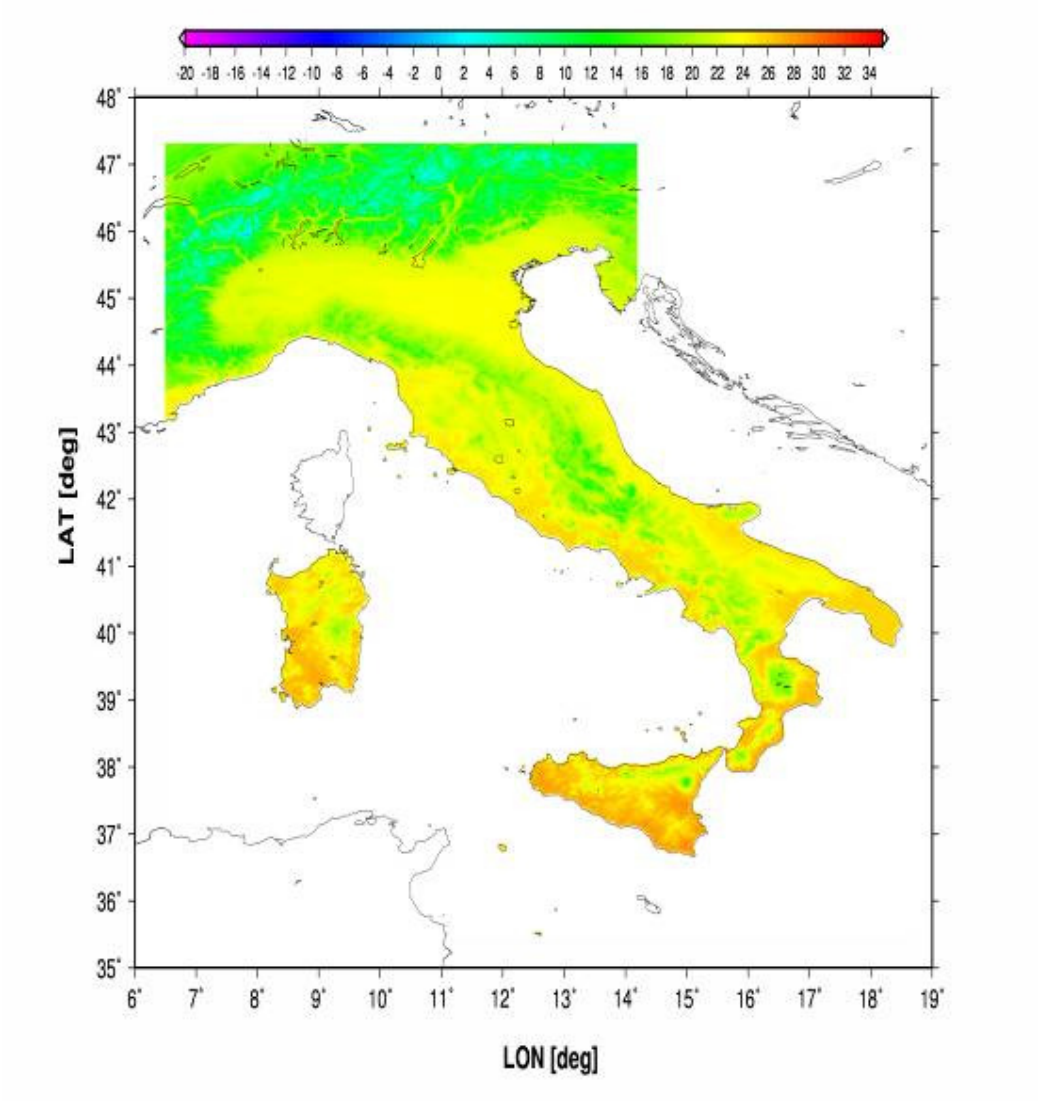

Fig.55 July1961-90 T_M map after top valley effect and all the former modelled effects (°C)

• Minimum Temperature

The same methodology used for T_M was used for T_N, but coefficients are different, as we can see in table 26.

	a	b
JAN	0.99	-0.21
FEB	1.04	-0.23
MAR	0.94	-0.22
APR	0.97	-0.24
MAY	1.05	-0.30
JUN	1.20	-0.36
JUL	1.35	-0.42
AUG	1.40	-0.44
SEP	1.24	-0.37
OCT	1.20	-0.34
NOV	0.98	-0.24
DEC	0.87	-0.17

Tab.26 Monthly coefficients for macro-aspect model for T_N

Also for T_N an "isolated summit" is subjected to a warming effect of, e.g. 0.98 °C in July, whilst a "pothole valley" is subjected to a cooling effect of, e.g., -0.42 °C in the same month.

+ Maximum Temperature

The same methodology used for T_M and T_N was used for T_X, but coefficients are different:

	a	b
JAN	-0.84	0.38
FEB	-1.04	0.42
MAR	-1.09	0.39
APR	-0.99	0.33
MAY	-0.88	0.32
JUN	-0.80	0.30
JUL	-0.83	0.33
AUG	-0.79	0.34
SEP	-0.90	0.34
OCT	-0.92	0.36
NOV	-0.82	0.34
DEC	-0.56	0.28

Tab.27 Monthly coefficients for macro-aspect model for T_X

For T_X the situation is opposite in comparison with T_N and T_M. In fact, an "isolated summit" is subjected to a cooling effect of, e.g. -0.5 °C in July, whilst a "pothole valley" is subjected to a warming effect of, e.g., 0.33 °C in the same month.

- **Improvements and evaluation of the Residuals after summit-valley effect**

Once again, residuals were calculated as:

$$RESTM_{MLR+SEA+LAKE+PO+SUN+ASP+TV} = RESTM_{MLR+SEA+LAKE+PO+SUN+ASP} - TV_M \quad (95)$$

The same holds for T_N and T_X.

In the next table we show the statistical parameters in °C:

After Top-Valley	YEAR	-0.02	1.08	1.37	YEAR	-0.01	0.83	1.05	YEAR	-0.07	1.03	1.34
After Macro-Aspect	YEAR	-0.06	1.10	1.40	YEAR	-0.02	0.83	1.06	YEAR	0.07	1.04	1.35
IMPROVEMENT	YEAR	0.04	0.02	0.03	YEAR	0.01	0.00	0.01	YEAR	0.00	0.01	0.01

Tab.28 Yearly averaged statistical error values after top-valley corrections and comparisons (°C)

The *LR* model used for top valley effects improves the statistical errors, especially for the T_N model, if we consider that other 6 effects were already de-trended from data. A threshold top-valley effect was used in *Hiebl et al.* (2009) and in *Brunetti et al. (2009)*, but the *LR* model performs better for the Italian territory.

4.3.9 Step 8 (Global improvement): land cover and urban heat island

+ Land cover grid: Land Cover raster from *GLC2000* Land Cover grid

Many local-scale or micro-scale time-space climate studies on temperature versus land cover (e.g. *Gallo et al., 1996; Shudo et al., 1997; Dong et al., 1998; Huang et al., 2007; Lim*

et al., 2008) can be found in literature, especially in China and in the USA. However, land cover variables are rarely used in global or regional scale climatologies.

We used the *GLC2000* land cover *(JRC website)* raster, see Chapter 4.3.4 for details, and we assigned to each station the corresponding land cover class.

Within this classification, our T_M stations are thus subdivided:

Mosaic: Tree Cover / Other natural vegetation	***1***
Snow and Ice	***3***
Irrigated Agriculture	***4***
Bare Areas	***9***
Mosaic: Cropland / Shrub and/or grass cover	***26***
Sparse herbaceous or sparse shrub cover	***27***
Shrub Cover, closed-open, deciduous	***39***
Shrub Cover, closed-open, evergreen	***88***
Herbaceous Cover, closed-open	***104***
Tree Cover, mixed leaf type	***104***
Tree Cover, needle-leaved, evergreen	***229***
Artificial surfaces and associated areas	***224***
Tree Cover, broadleaved, deciduous, closed	***333***
Cultivated and managed areas	***290***

Tab.29 Number of T_M stations per land cover class

Let us show some single class examples:

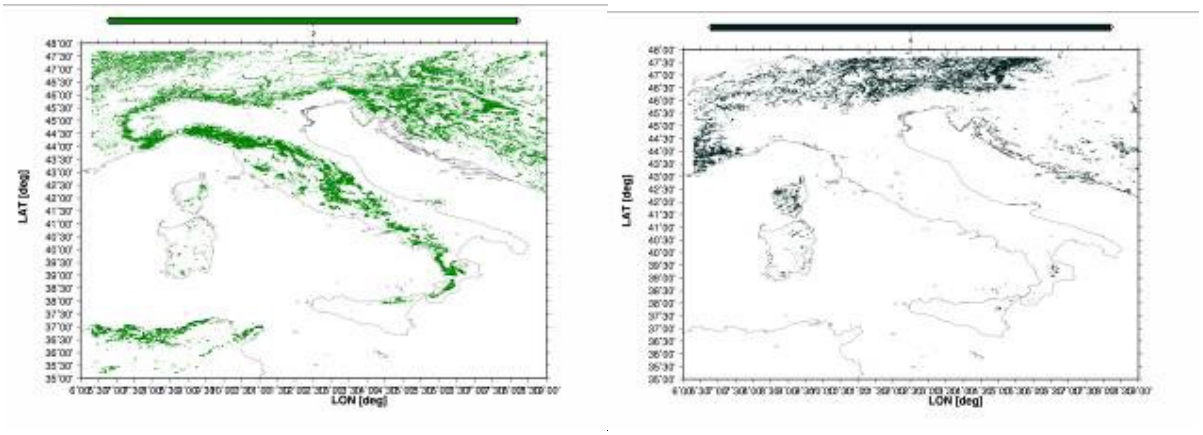

Fig.56-57 Left: broadleaved deciduous closed tree cover; right: needle leaved evergreen tree cover

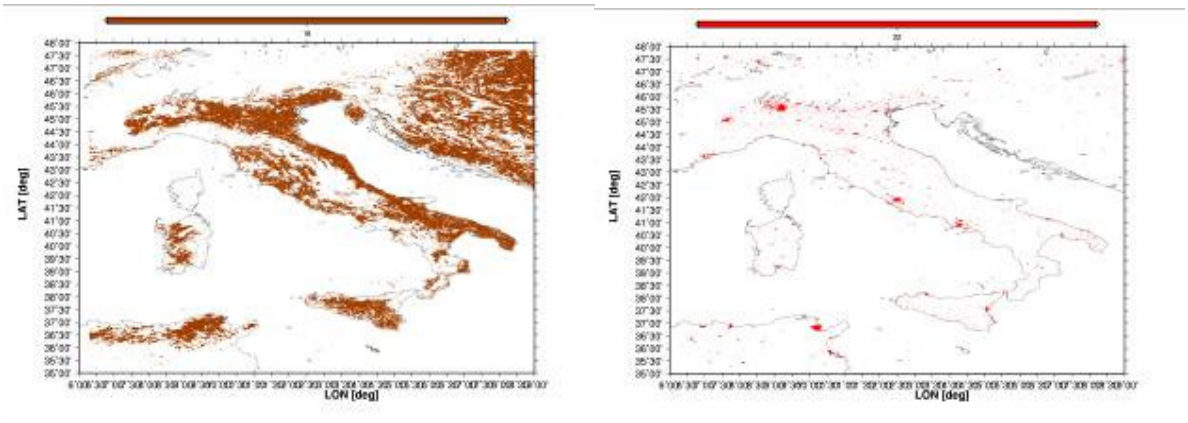

Fig.58-59 Left: cultivated and managed areas; right: artificial surfaces and associated areas

By means of Google Earth™ we checked, for example, whether the stations are actually in forest areas if they are assigned a "tree cover" land cover class. We discovered that, because of the inadequate land cover scale (a 50 m scale would be good), only stations labelled as "artificial areas" are in the majority of cases (approximately 90%) inopportunely labelled, thus we decided to use only this land cover class as a predictor.

The red cells (see fig. 59), i.e. the "artificial surfaces" stations, were studied in order to model the so-called *UHI* (Urban Heat Island), which is a very local and very important phenomenon.

The labelling of the *GLC2000* is probably too fine for our purposes. Thus a better resolution land cover grid and a correct geo-referenced set of stations would probably, in the future, lead to the modelling of difference behaviour of, e.g., forested areas and cultivated areas or bare area versus shrubs, crops or grass fields. Nevertheless, such differences are very local in space and time, thus in a macro-region and in a 30-year interval, these effects would yield very smoothed results.

• Preliminary comments on *UHI* effect (a short bibliographic review)

The urban heat island is an anthropogenic phenomenon which appears in urban areas. It is due to an increased absorption of short wave radiation due to canyon geometry, a decrease of outgoing radiation (caused by a reduction of the sky view factor), artificial heat sources, an increased sensible heat (that is enthalpy in this case) storage, a decreased evapotranspiration due to construction materials, a decreased total turbulent heat transport caused by a wind speed reduction in a narrow canyon geometry city and so on

(Oke, 1982). Meteorological conditions can favour the formation of *UHI*, which is strong especially in calm and cloudless winter nights *(Landsberg, 1981; Kim et al., 2002)*, thus T_N should be more affected.

In climate studies, *UHI* was modelled versus many predictors: population, canyon sky view geometry, thermal conductance; in any case, it is well known that *UHI* is a micro-scale effect *(Oke, 1976; Oke, 1982; Karl et al., 1988; Oke , 2004)*.

In literature, it is easy to find studies dedicated to the removal of *UHI* effect in temperature trends, for T_M in China by *Li et al. (2004)* or *Portman (1993)*. *Hua et al. (2007)* found *UHI* up to 0.74 °C in large cities in China, in other countries by, e.g., *Camilloni et al. (1997)*, comparing 1951-1980 and 1971-2000 averages. (*Chung et al., 2004b)* found *UHI* up to 0.5 °C in night-time data in south-eastern Asia. In global trends, *Karl et al. (1989)* found that T_N are increased by *UHI*, whilst T_X are decreased. *Jones et al. (1988)* found that *UHI* increases T_M by *0*.1 °C in the Northern Hemisphere in 1900-1980. *Kukla et al. (1986)* found that *UHI* increases T_M by 0.12 °C/10y in northern USA and *Karl et al. (1988)* found a similar value, i.e., 0.16 °C in the US in 1901-84.

One common methodology used to detect *UHI* locally is based on the comparison of urban versus rural stations: such studies have been performed in Hyogo by *Aikawa et al. (2008a)*, in New York by *Gaffin et al. (2008)*. In Fairbanks, Alaska, *Magee et al (1999)* found a mean *UHI* of 0.4 °C, up to 1.0 °C in winter. In Seoul *Kim et al. (2002)* found a mean *UHI* of 0.56 °C. In Melbourne *Morris et al. (2000)* found a *UHI* of 1.13 °C. In Barcelona *Moreno-Garcia (1994)* found a *UHI* of 2.9 °C for T_N and -0.2 °C for T_X. In Beijing *Liu et al. (2008)* found a mean yearly *UHI* of 1.76 °C in 1971-2003. In GAR, *Hiebl et al. (2009)* found a *UHI* of 1.5 °C in cities with more than 1 million inhabitants. In Vienna, *Böhm (1998)* found a mean *UHI* varying from 0.2 °C to 1.6 °C, depending on the location.

Even though in some cases (*Peterson, 2003)* no differences between urban and rural station data were found, *UHI* can show high daily values. For example, in Lodz it reaches 8.0 °C on calm nights *(Klysik et al., 1999)*, in Melbourne it ranges from -3.2 °C to 6.0 °C *(Morris et al., 2000)*. Many other examples can be found in *Peterson (2003)*.

In spatial climatologies *UHI* is rarely modelled, even if it can improve (up to 30% for *Choi et al. (2003)*, even though in our opinion this value is too high) considerably the statistical parameters, above all in regional climatologies in highly urbanized areas (e.g., the Shangai region).

For Italy, *Ferretti et al. (1993)* found a *UHI* in Milan (large city) of 2.2 °C for T_N, of 1.1 °C for T_M and of 0.1 °C for T_X. *Pangallo et al. (2004)* found a *UHI* in Milan of 1.5 °C for T_N, of 0.8 °C for T_M, null for T_X. The same authors reported a *UHI* in Lodi (medium city) of 0.9 °C

for T_N, of 0.3 °C for T_M and of -0.2 °C for T_X and a *UHI* in Paullo (small city) of 0.2 °C for T_N, of -0.2 °C for T_M and of -0.2 °C for T_X,

Thus, it seems that *UHI* is a micro-scale phenomenon that involves more T_N than T_M, whilst it can cause a decrease in T_X because of shadowing geometries in city centres.

• Mean Temperature (*UHI*)

We decided to evaluate the monthly residual (from equation (95)) of the 224 T_M stations labelled with "artificial surfaces and associated areas" and we averaged their values, thus we modelled *UHI* as:

$$UHI_M = \overline{RESTM_S}(LCOV_{ARTIFICIALSURFACES})\Big|_{eq.95} \quad \textbf{(96)}$$

The *UHI* values used in T_M model, in °C, are:

JAN	0.40
FEB	0.28
MAR	0.14
APR	0.05
MAY	0.06
JUN	0.05
JUL	0.08
AUG	0.12
SEP	0.19
OCT	0.32
NOV	0.31
DEC	0.45

Tab.30 UHI coefficients for T_M (in °C)

As expected, the *UHI* is stronger in winter than in summer, where it almost vanishes.

In the end, we added back the *UHI* effects to the T_M modelled with *MLR* plus sea, lake, solar radiation, macro-aspect, and summit-valley effects as:

$$TM8_M = TM7_M + UHI_M \quad \textbf{(97)}$$

• Minimum Temperature (*UHI*)

The same methodology used for T_M was used for T_N, we used 204 T_N stations labelled and the *UHI* values used in T_N model are:

JAN	0.29
FEB	0.26
MAR	0.16
APR	0.08
MAY	0.12
JUN	0.15
JUL	0.22
AUG	0.27
SEP	0.31
OCT	0.39
NOV	0.31
DEC	0.29

Tab.31 UHI coefficients for T_N (°C)

As expected, the *UHI* is stronger in winter than in summer, but it is less intense than for T_M.

• Maximum Temperature (*UHI*)

The same considerations made for T_N are valid for T_X, the *UHI* values used in T_X model are:

JAN	0.16
FEB	0.04
MAR	-0.08
APR	-0.19
MAY	-0.24
JUN	-0.32
JUL	-0.36
AUG	-0.37
SEP	-0.18
OCT	0.06
NOV	0.05
DEC	0.24

Tab.32 UHI coefficients for T_X (°C)

As expected, the *UHI* is negative in summer, and the year cycle of Tx urban heat islands (negative in summer, positive in winter) is well documented in literature.

Coefficients are physically based, not only a statistical average, thus the *UHI* is satisfactorily modelled in Temperature models for Italy.

• Other land cover effects not modelled

It can be worth listing the averaged residuals (in °C) for the other land cover classes, calculated as the average of the residuals from equation (95) for the stations which belong to each particular land cover class.

LCOV CLASS	STAZ	MED JAN	MED FEB	MED MAR	MED APR	MED MAY	MED JUN	MED JUL	MED AUG	MED SEP	MED OCT	MED NOV	MED DEC	MED YEAR
Mosaic: Tree Cover / Other natural vegetation	1	-0.04	0.02	0.23	0.20	0.31	0.34	0.34	0.12	0.18	0.07	0.11	0.15	0.17
Snow and Ice	3	-1.37	-0.71	-0.71	-0.72	-0.47	-0.85	-1.22	-0.96	-0.74	-0.61	-1.09	-1.15	-0.88
Irrigated Agriculture	4	-0.07	-0.11	0.03	0.10	0.19	-0.02	-0.17	-0.22	-0.31	-0.16	-0.18	-0.09	-0.08
Bare Areas	9	-0.50	-0.35	-0.16	-0.12	-0.09	-0.11	-0.18	-0.22	-0.23	-0.30	-0.46	-0.51	-0.27
Mosaic: Cropland / Shrub and/or grass cover	26	0.20	0.24	0.17	0.10	0.11	0.02	0.02	0.02	0.06	0.16	0.14	0.20	0.12
Sparse herbaceous or sparse shrub cover	27	-0.32	-0.22	-0.31	-0.44	-0.49	-0.49	-0.34	-0.23	-0.14	-0.03	-0.17	-0.22	-0.28
Shrub Cover, closed-open, deciduous	39	-0.06	-0.09	0.04	0.09	0.15	0.18	0.17	0.15	0.11	-0.02	-0.04	-0.09	0.05
Shrub Cover, closed-open, evergreen	88	0.14	0.09	0.06	0.05	0.05	0.05	0.05	0.04	0.08	0.14	0.14	0.14	0.09
Herbaceous Cover, closed-open	104	0.23	0.09	-0.04	-0.09	-0.11	-0.09	-0.07	-0.04	0.06	0.16	0.22	0.28	0.05
Tree Cover, mixed leaf type	104	-0.15	-0.17	-0.14	-0.12	-0.15	-0.14	-0.14	-0.15	-0.21	-0.21	-0.20	-0.19	-0.16
Tree Cover, needle-leaved, evergreen	229	-0.07	-0.09	-0.10	-0.06	-0.03	-0.04	-0.04	-0.03	-0.04	-0.04	-0.03	-0.05	-0.05
Artificial surfaces and associated areas	224	0.40	0.28	0.14	0.05	0.06	0.05	0.08	0.12	0.19	0.32	0.31	0.45	0.20
Tree Cover, broadleaved, deciduous, closed	333	-0.04	-0.02	-0.01	0.00	-0.01	-0.03	-0.06	-0.07	-0.07	-0.08	-0.05	-0.07	-0.04
Cultivated and managed areas	290	0.08	0.06	0.03	0.00	0.00	0.02	0.05	0.06	0.07	0.08	0.08	0.09	0.05

Tab.33 Average residuals by land cover classes for mean temperatures (°C)

In TM, rice fields (Piedmont or Piemonte) seems to show negative residuals, but 4 stations are not enough to provide reliable coefficients. Bare areas (high mountain areas without vegetation) seem to show negative residuals, especially in winter (up to -0.5 °C), as sparse herbaceous or shrub areas, which are similar areas. Such effects should be further studied in future. Other shrub, grass and crop areas show low positive or low negative residuals. Tree covered areas are negatively biased; this would be another

interesting effect but it should be better investigated in the future. Cultivated areas show quite null residuals.

Such coefficients were not used in models because they should be deeper analyzed and because the station subset was not statistically large enough and/or the effect was not completely justified by physical explanations.

- **Improvements and evaluation of the Residuals after *UHI* effect**

Once again, residuals were calculated as:

$$RESTM_{MLR+SEA+LAKE+PO+SUN+ASP+TV+UHI} = RESTM_{MLR+SEA+LAKE+PO+SUN+ASP+TV} - UHI_M \quad (98)$$

The same holds for T_N and T_X.

In table 34 we show the statistical parameters about errors after this step.

		ME	MAE	RMSE		ME	MAE	RMSE		ME	MAE	RMSE
	JAN	0.00	1.21	1.55	JAN	0.05	1.01	1.29	JAN	0.04	1.13	1.46
	FEB	-0.05	1.11	1.43	FEB	-0.02	0.83	1.07	FEB	-0.01	1.01	1.33
	MAR	-0.08	0.99	1.27	MAR	-0.07	0.74	0.95	MAR	-0.06	0.92	1.23
	APR	-0.11	0.97	1.24	APR	-0.10	0.75	0.95	APR	-0.09	0.93	1.22
	MAY	-0.12	1.00	1.27	MAY	-0.10	0.74	0.94	MAY	-0.13	0.97	1.26
	JUN	-0.13	1.07	1.35	JUN	-0.11	0.81	1.01	JUN	-0.15	1.06	1.36
	JUL	-0.11	1.17	1.47	JUL	-0.10	0.87	1.10	JUL	-0.14	1.13	1.44
	AUG	-0.09	1.13	1.42	AUG	-0.08	0.84	1.06	AUG	-0.13	1.11	1.40
	SEP	-0.05	1.04	1.31	SEP	-0.04	0.75	0.95	SEP	-0.05	1.02	1.31
	OCT	-0.01	1.02	1.27	OCT	0.01	0.74	0.95	OCT	0.00	0.99	1.28
	NOV	0.00	1.03	1.30	NOV	0.04	0.80	1.03	NOV	0.02	0.96	1.26
	DEC	0.00	1.18	1.49	DEC	0.06	1.01	1.29	DEC	0.06	1.12	1.45
After UHI	YEAR	-0.06	1.08	1.36	YEAR	-0.04	0.82	1.05	YEAR	-0.05	1.03	1.33
After T-V	YEAR	-0.02	1.08	1.37	YEAR	-0.01	0.83	1.05	YEAR	-0.07	1.03	1.34
IMPROVEMENT	YEAR	0.00	0.00	0.01	YEAR	-0.04	0.01	0.00	YEAR	0.02	0.00	0.01

Tab.34 Monthly statistical error values after UHI corrections and comparisons (°C)

Now, let us show a comparison of errors after *MLR* and once all the local and global improvements were modelled.

After Step 8	***YEAR***	***-0.06***	***1.08***	***1.36***		***YEAR***	***-0.04***	***0.82***	***1.05***		***YEAR***	***-0.05***	***1.03***	***1.33***
After MLR	***YEAR***	***0.19***	***1.19***	***1.51***		***YEAR***	***0.06***	***0.92***	***1.17***		***YEAR***	***-0.11***	***1.20***	***1.53***
IMPROVEMENT	***YEAR***	***0.13***	***0.11***	***0.15***		***YEAR***	***0.02***	***0.10***	***0.12***		***YEAR***	***0.06***	***0.17***	***0.20***

Tab.35 Yearly statistical error values after MLR and after improvements (°C)

The seven modelled effect after *MLR* led to meaningful improvements in statistical errors. The average *MAE* was decreased by 0.11 °C for T_N, by 0.10 °C for T_M and by 0.17 °C for T_X, while the average *RMSE* was diminished by 0.15 °C for T_N, by 0.12 °C for T_M and by 0.20 °C for T_X. At this point, for T_M, 10 out of 12 months are under the error threshold of 1.0 °C for the *MAE*, 2 out of 12 months for T_N and 5 out of 12 months for T_X.

Let us show the residual maps for T_N for January and July.

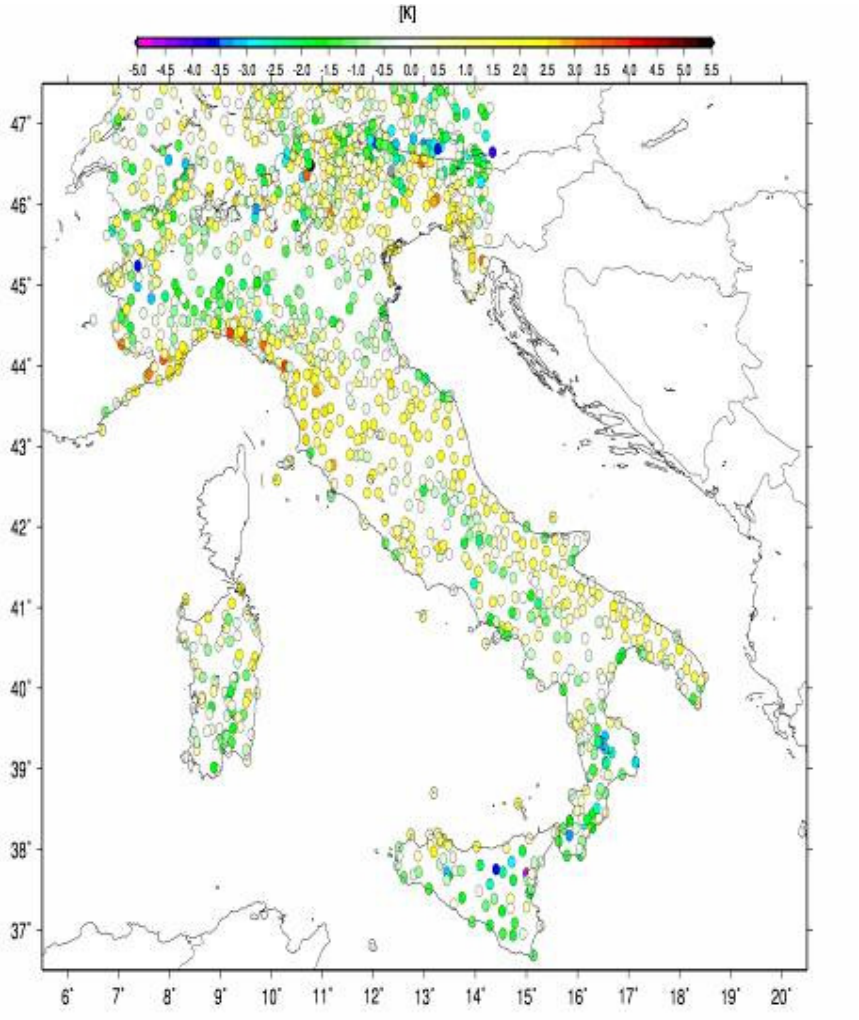

Fig.60 January map of T_M residuals after local and global improvements

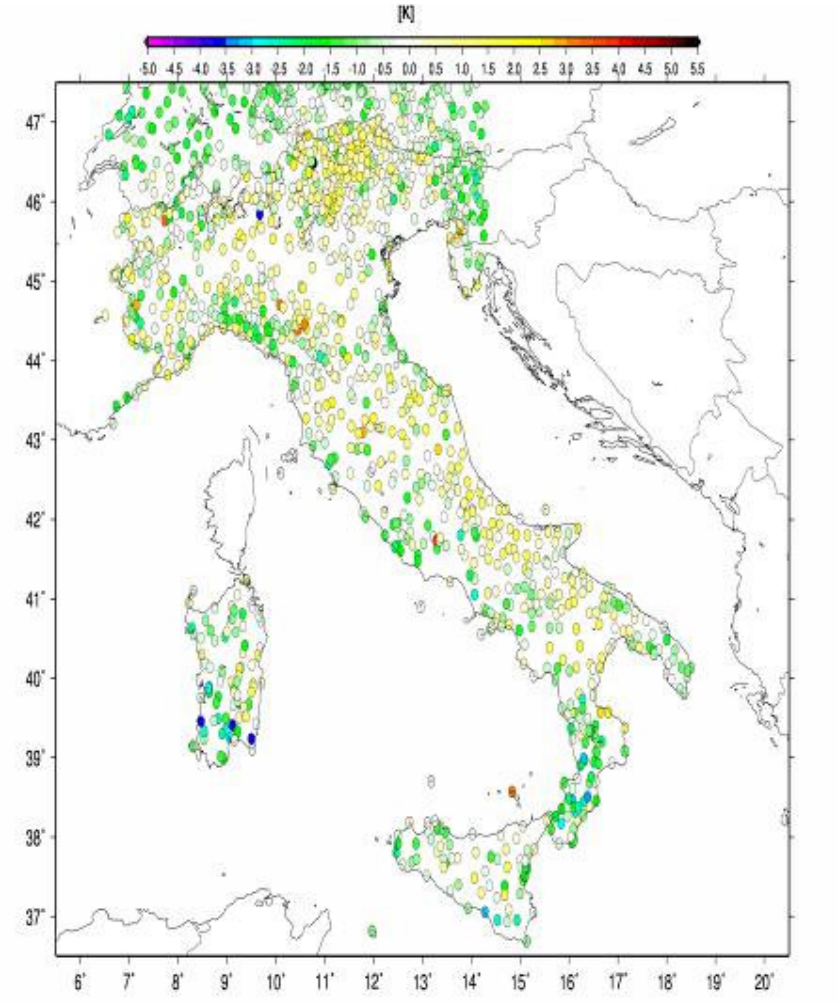

Fig.61 July map of T_M residuals after local and global improvements

If we compare fig. 60 with fig. 35, i.e. January residuals after *MLR* and after the 7 improvements, we can easily see that the situation was improved, even though there are still some biased regions, e.g., Liguria, southern Sicily and the Italian border near Slovenia. Similar considerations can be made comparing fig. 61 with fig. 36, i.e. July residuals. Residuals show local or regional common features; thus, an inverse distance weighting model to study the stochastic part is a good choice to improve our models, as we can see in the next paragraph.